A comparison of computed tomography imaging with histopathology in the sensitivity and correlation of evaluating coronary arterial calcification

Yun-Fei Liu[1,2], Yan-He Ma[3], Chang-Yue Wang[4], Xiang-Li Zhang[1,2], Ke-Ke Liang[1,2], Jing Tao[5], Lin Guo[1], Bu-Lang Gao[1]

[1]Department of Critical Care Medicine, Zhengzhou Seventh People's Hospital, Zhengzhou, China; [2]Department of Heart Transplantation Center, The First Affiliated Hospital of Zhengzhou University, Zhengzhou, China; [3]Department of Radiology, Tianjin Chest Hospital, Tianjin, China; [4]Department of Anatomy and Histoembryology, Tianjin Medical University, Tianjin, China; [5]Pathological Department, Henan Provincial Children's Hospital, Zhengzhou, China

Contributions: (I) Conception and design: YF Liu, YH Ma, CY Wang; (II) Administrative support: YH Ma, CY Wang; (III) Provision of study materials or patients: YF Liu, YH Ma, CY Wang, XL Zhang, KK Liang, J Tao, L Guo; (IV) Collection and assembly of data: All authors; (V) Data analysis and interpretation: YF Liu, BL Gao; (VI) Manuscript writing: All authors; (VII) Final approval of manuscript: All authors.

Correspondence to: Xiang-Li Zhang. Department of Heart Transplantation Center, The First Affiliated Hospital of Zhengzhou University, No. 1 Jianshe East Road, Zhengzhou 450052, China. Email: zxl1638@163.com; Lin Guo. Department of Critical Care Medicine, Zhengzhou Seventh People's Hospital, 17 Jingnan Fifth Road, Zhengzhou Economic and Technological Development Zone, Zhengzhou 450016, China. Email: 13653829203@163.com.

Background: The sensitivity and correlation of coronary computed tomography angiography (CTA) as compared with histopathology are unknown in evaluating coronary arterial calcification. In this study, we retrospectively evaluated qualitatively and quantitatively the sensitivity and correlation of coronary CTA compared with histopathology in assessing coronary arterial calcification.

Methods: This study was conducted on 12 randomly selected cadavers aged over 40 years at the time of death, and 53 segments of coronary arteries from these 12 cadavers were obtained from the Human Anatomy Laboratory of Tianjin Medical University. The artery segments were scanned using contrasted-enhanced dual-source computed tomography (DSCT) with an axial slice thickness of 0.6 mm. Coronary artery calcification in a coronary segment was defined as the presence of 1 or more voxels with a CT density >130 Hounsfield units. According to the arc of calcification in the cross section of the coronary artery wall, calcified plaques were divided into three categories: mild, moderate, and severe calcification. The coronary artery stenosis caused by calcified plaque was observed and calculated with multiplanar reconstruction (MPR), maximum density projection, volume rendering (VR), and cross-sectional reconstruction. After CT enhancement scanning, the coronary artery specimens were cut into 4-mm long segments and embedded in paraffin for pathological staining. Pathological classification and coronary artery stenosis measured with pathological analysis were used as comparison criteria.

Results: Histopathology detected 69 Vb-type plaques, while DSCT detected 57 calcified plaques. The sensitivity of CT for detecting mild, moderate, and severe calcified plaques were 88.3% [95% confidence interval (CI): 74.1–95.6%], 100% (95% CI: 69.8–100%), and 100% (95% CI: 73.2–100%), respectively. DSCT had a significant ($P<0.001$) correlation with histopathology in quantifying coronary artery stenosis caused by mild, moderate, and severe calcified plaques ($R^2=0.9278$, $R^2=0.9158$, $R^2=0.7923$, respectively). Compared with histopathology, DSCT overestimated coronary artery stenosis caused by mild, moderate, and severe calcified plaques (3.2%±2.0%, 4.9%±4.7%, and 14.7%±8.2%, respectively; $P<0.05$).

Conclusions: DSCT contrast enhancement scanning can detect and characterize coronary artery calcification with a good correlation with histopathologic quantification of coronary artery stenosis caused by different types of calcified plaques, even though coronary CTA may overestimate the stenosis.

Keywords: Coronary artery calcification; computed tomography; stenosis; histopathology

Introduction

Calcification of the coronary artery is a significant independent risk factor in predicting cardiac events and death in patients with coronary heart disease (1-5). Microcalcification, spotty calcification, and calcified nodules are closely related to acute coronary syndrome (6-9). Severe coronary artery calcification often indicates a heavy burden of coronary atherosclerotic plaque, which is closely related to stable angina pectoris (10,11). Moreover, severe, extensive, and diffuse coronary artery calcification will increase the risk of percutaneous coronary intervention and coronary artery bypass grafting as well as the poor prognosis of patients (12-15). Therefore, accurate qualitative and quantitative evaluation of coronary artery calcification is of great clinical significance to guide the classification, treatment, and prognosis of patients with coronary heart disease. Dual-source computed tomography (DSCT) with high temporal and spatial resolution and advanced postprocessing technology can qualitatively and quantitatively assess coronary artery calcified plaques (16,17); however, the relevant literature suggests it lacks pathological control. It was hypothesized that DSCT could qualitatively and quantitatively assess the coronary artery calcified plaques based on the histopathological evaluating outcomes. This study was consequently performed to compare DSCT imaging with histopathological outcomes in detecting coronary artery calcified plaques. We present the following article in accordance with the STARD reporting checklist (available at https://qims.amegroups.com/article/view/10.21037/qims-22-603/rc).

Methods

Coronary arteries

The study was conducted in accordance with the Declaration of Helsinki (as revised in 2013). This retrospective study was approved by the ethics committee of The First Affiliated Hospital of Zhengzhou University (No. 20201252), and individual consent for this retrospective analysis was waived. From January 2013 to June 2015, this study was performed on 12 randomly selected cadavers older than 40 years old at the time of death from the Human Anatomy Laboratory of Tianjin Medical University for research (*Figure 1*). The causes of death were lung cancer, renal failure, myocardial infarction, liver cancer, chronic obstructive pulmonary disease, left heart failure, rectal cancer, breast cancer, myocardial infarction, liver rupture, cerebral infarction, and cervical cancer. All the corpses were voluntarily donated and soaked in formalin for teaching and scientific research. The medical history, the presence of coronary arterial calcification, and risk factors for cardiac diseases of each specimen were not recorded in detail. The coronary specimens of humans were obtained from 12 autopsied patients, including 7 males and 5 females with an age range of 42–80 (mean 67.5±10.2) years at death. The hearts were fixed with 10% formalin. The right coronary artery, left main trunk, anterior descending branch, and left circumflex branch on the surface of the heart were dissected. Small branches and ends of the vessels were ligated. The coronary artery was cut off from the beginning, the fatty tissue around the arteries was removed, and the arteries were washed with physiological saline water 3 times. Coronary arteries with wall damage and lumen obstruction were excluded.

A 5-mL syringe connected to a catheter was used to inject contrast medium [the contrast medium consisted of 350 mg/mL of iohexol and normal saline in a ratio of 1:40 and a CT value of 280 Houndsfield units (HU)] into the coronary artery from the upper opening of the coronary artery, which was to obtain the enhancement effect similar to that in clinical CT examination. The coronary artery was
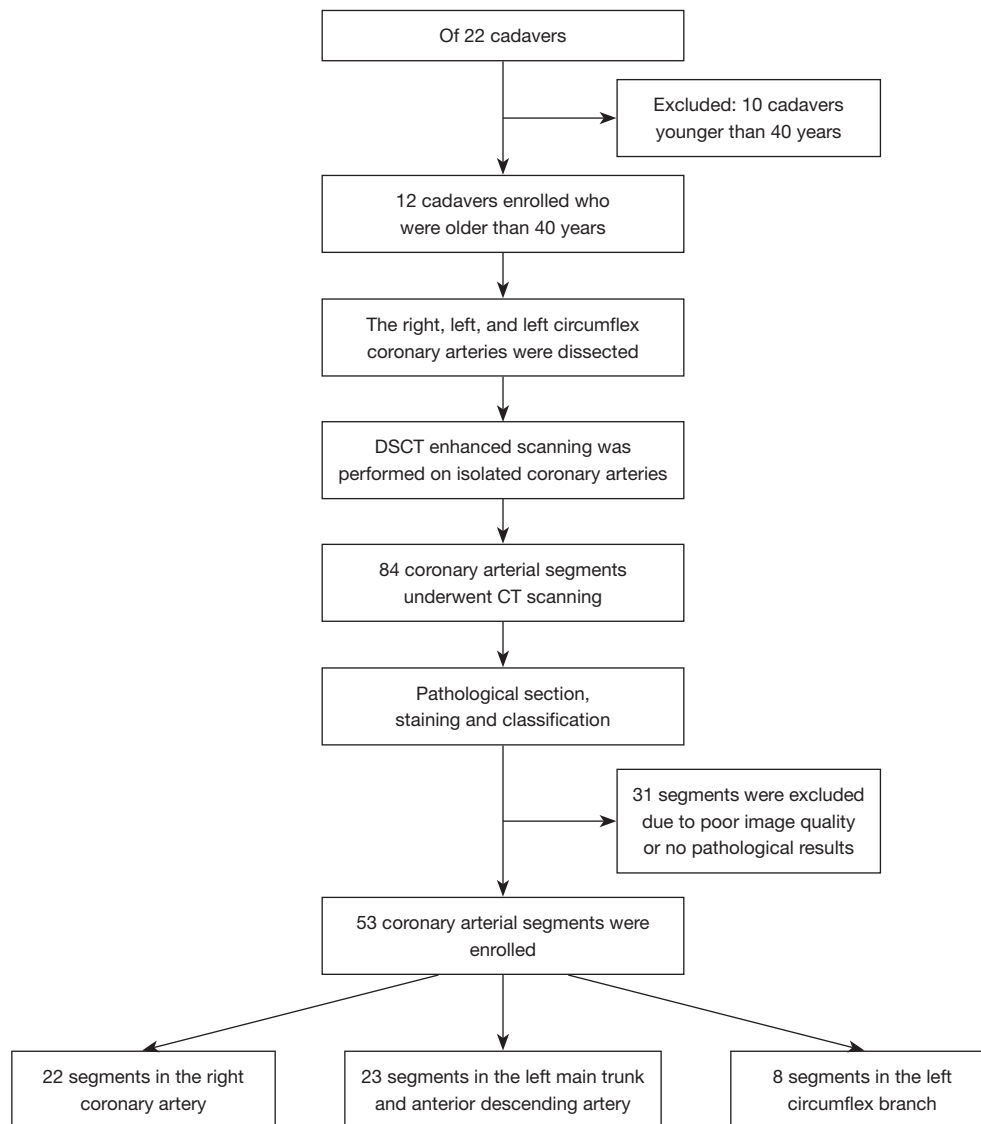
Figure 1 Flowchart of specimen inclusion. DSCT, dual-source computed tomography; CT, computed tomography.

placed on a plate at a certain angle on the scanning table to prevent the contrast medium from flowing out. The long axis of the coronary artery was consistent with the long axis of the bed, similar to the position in the cardiac cavity. A 5-mL syringe was filled with contrast medium and placed on one side of the coronary artery for comparison and localization. In this study, only the isolated coronary artery with a smooth lumen was scanned, and the *in vitro* coronary scanning was completed at 37 ℃ room temperature. After enhanced scanning, the contrast medium in the coronary

artery was sucked out and washed with normal saline 3 times to prevent the contrast agent from sticking to the vessel wall and affecting further pathological sections.

CT scanning

CT scanning was performed with the dual source 64-slice SOMATOM CT scanner (Somatom Definition; Siemens Healthineers, Erlangen, Germany) in Tianjin Chest Hospital under the following parameters: tube voltage,
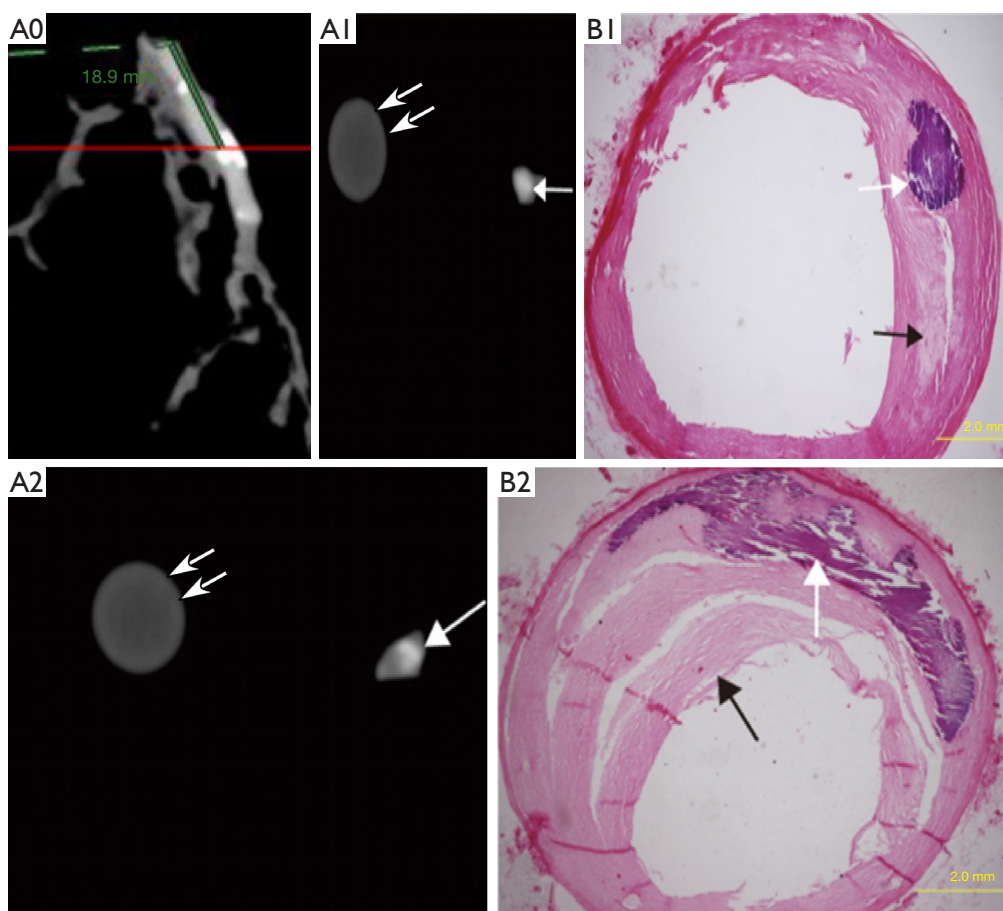
Figure 2 Calcified plaques of the coronary artery (arrows) as shown in CT MIP (A0) and cross-sectional imaging (A1–2) and histopathology (B1–2; hematoxylin and eosin staining, ×40). (A0) The distance of the plaque to the coronary ostium was measured with the MIP reconstruction. (A1) Mildly calcified coronary plaques (single white arrow) are shown on the cross-sectional image. (B1) Mildly calcified coronary plaques (single white arrow) are shown in the histopathological section. The coronary artery stenosis quantified with the dual-source CT and histopathologic staining was 38% and 36%, respectively. The black arrow shows lipid deposition. In A1, the single arrow indicates the calcium, and the double arrows indicate the cross section of a 5-mL syringe. (A2) Moderately calcified coronary plaques (white arrow) appear on the cross-sectional imaging. (B2) Moderately calcified coronary plaques (white arrow) are shown in the histopathological section. The coronary artery stenosis quantified with dual-source CT and histopathologic staining was 59% and 55%, respectively. The black arrow indicates the thick fibrous cap. The dual-source CT could not determine or quantify the thick fibrous cap. Double arrows indicate the cross section of a 5-mL syringe. CT, computed tomography; MIP, maximum intensity projection.

140 kV; tube current, 162 mA; field of view, 200 mm; rotation time, 0.33 s; pitch, 0.25; slice interval, 0.6 mm; and slice thickness, 0.6 mm.

Imaging process and measurement

The original CT images were transmitted to the Syngo VE32E workstation (Siemens Healthineers), and the maximum intensity projection (MIP), volume rendering (VR), and multiplanar reconstruction (MPR) were reconstructed for analysis of the coronary plaque (*Figures 2-4*). The distance of the plaque to the coronary artery orifice was measured with the MPR. Using the double-blinded method, 2 experimenters with 5 and 8 years of experience, respectively, read the images independently without knowing the histopathological outcome. When they disagreed, a third doctor with over 10 years of experience was consulted to reach a consensus. According to the American Heart
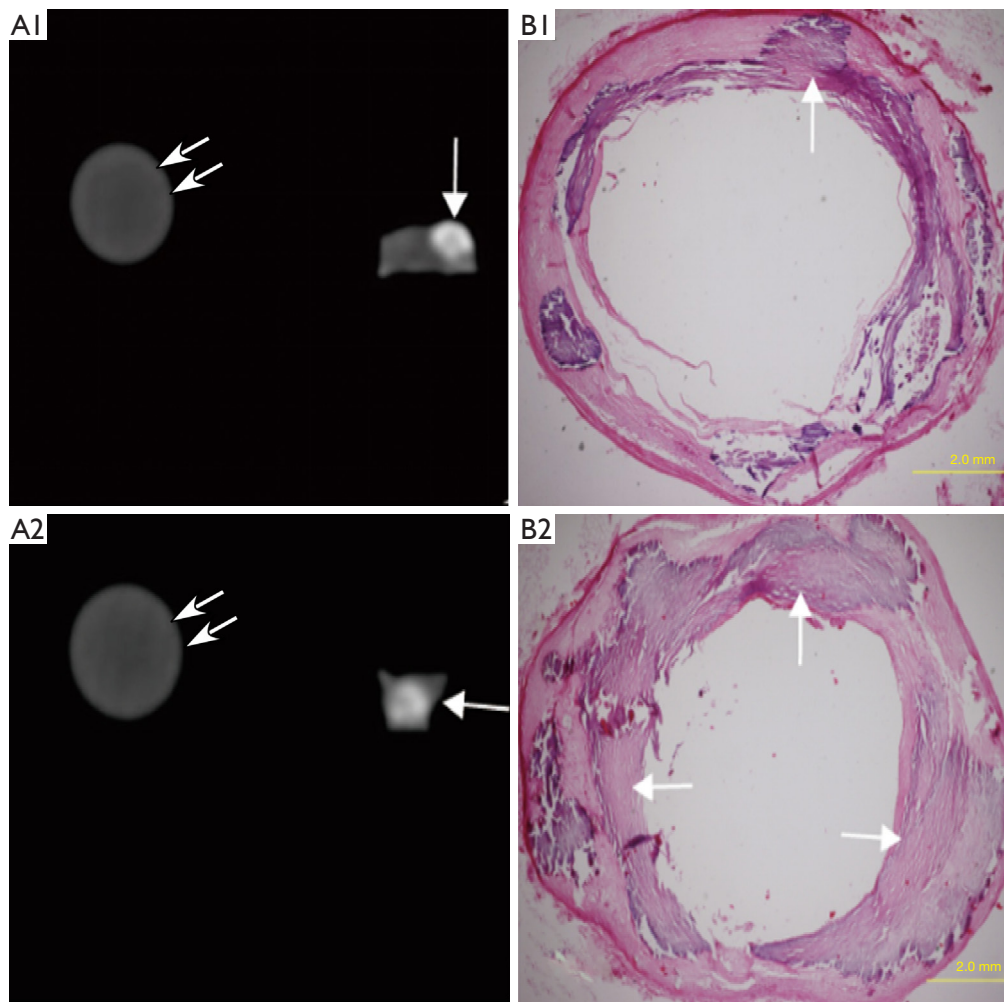
Figure 3 Severe calcified coronary artery plaques as shown on the cross-sectional imaging and histopathological staining (hematoxylin and eosin staining, ×40). (A1) Severe calcified coronary plaques (white arrow) are shown on the cross-sectional imaging. (B1) Severe calcified coronary plaques (white arrow) are shown on the histopathologic staining. The coronary stenosis quantified by histopathologic staining was 35%, and the severely calcified plaque did not cause severe stenosis but was wrongly diagnosed as obstructive coronary artery disease by DSCT. Double arrows indicate the cross section of a 5-mL syringe. (A2) Severely calcified plaques (white arrow) were shown on the cross-sectional imaging. (B2) Severely calcified plaques (white arrows) were shown on the histopathologic staining. The coronary stenosis quantified by DSCT and histopathologic staining was 73% and 52%, respectively. DSCT overestimated the coronary stenosis caused by severely calcified plaques. The double arrows indicate the cross section of a 5-mL syringe. DSCT, dual-source computed tomography.

Association (AHA) coronary artery segmentation standard (18), only larger coronary arteries (AHA1, 2, 3, 5, 6, 7, 8, 11, 12, and 13) were analyzed. Images with poor quality were excluded. When measuring the CT value of the plaque, the region of interest (ROI) was adjusted according to the size of the plaque. Each plaque was measured 3 times, and the average value was calculated. According to the results of previous studies (19,20), calcified plaques were defined as a CT value >130 HU. According to the arc or radian of calcification in the cross section of the arterial wall, calcified plaques were divided into 3 types (21,22): mild calcification, calcification arc <90°; moderate calcification, 90°< calcification arc <180°; and severe calcification, calcification arc >180°. Minute calcification belonged to the type of mild calcification. The three types of calcifications were also calculated.
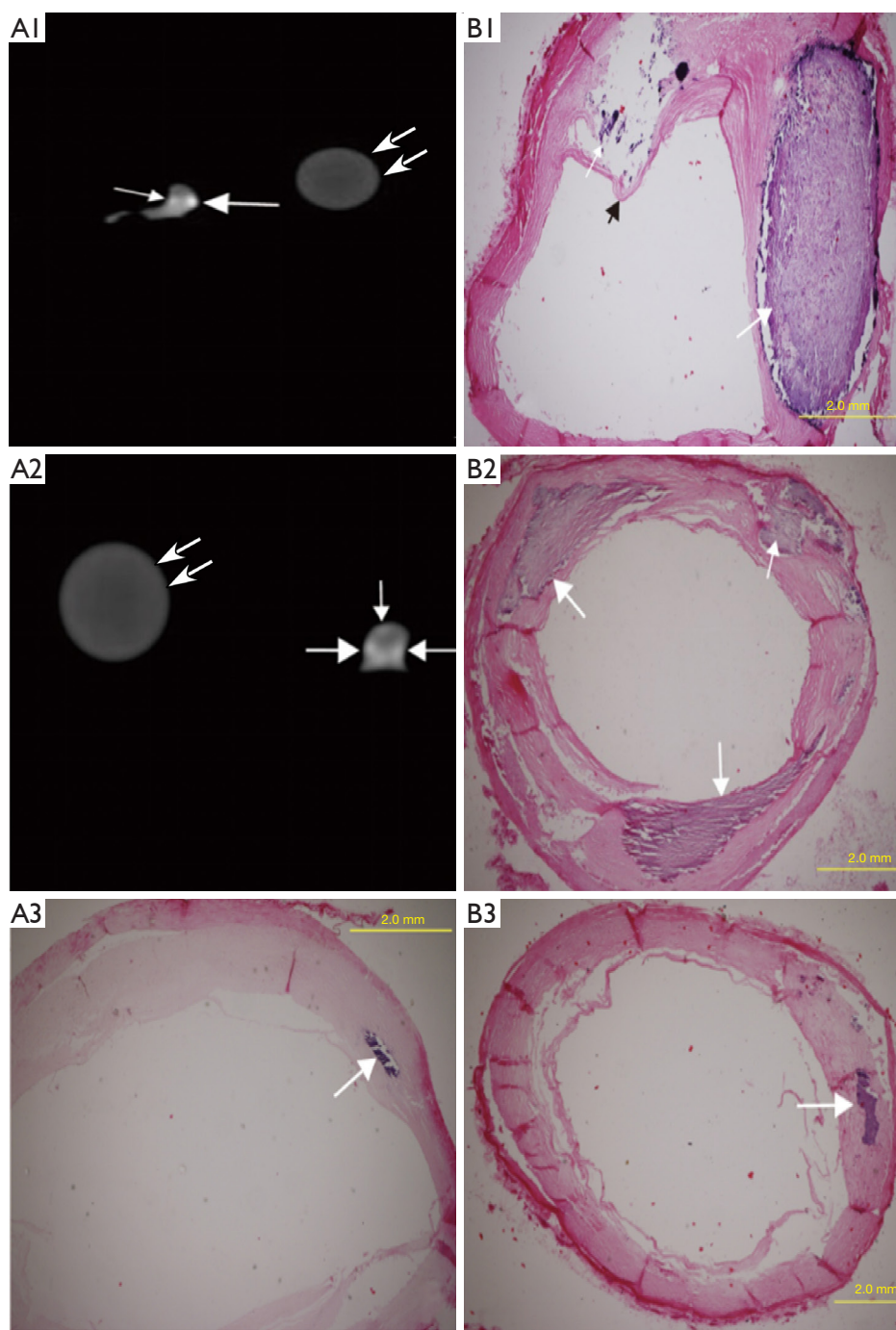
Figure 4 Two and three calcified plaques as shown on cross-sectional imaging and histopathologic staining (hematoxylin and eosin staining, ×40). (A1) Two calcified plaques (white arrow) are demonstrated on the cross-sectional imaging. (B1) Two calcified plaques (white arrows) are demonstrated on the histopathologic staining. The coronary stenosis quantified with DSCT and histopathologic staining was 68% and 53%, respectively. DSCT could not determine or quantify the thin fibrous cap (black arrow). Double arrows indicate the cross section of a 5-mL syringe. (A2) Three calcified plaques (white arrows) are shown on cross-sectional imaging. (B2) Three calcified plaques (white arrows) are shown on the histopathologic staining. DSCT indicating 3 calcified plaques. The two bigger arrows show the calcified plaques at the junction of intima and media, whereas the small arrow indicates the calcified plaque at the junction of media and adventitia. DSCT could not distinguish the location of calcified plaques in the coronary artery wall. (A3-B3) The 2 calcified plaques (white arrows) detected with histopathologic staining but not with DSCT. The double arrows indicate the cross section of a 5-mL syringe. DSCT, dual-source computed tomography.

In measuring coronary artery stenosis, MPR, MIP, VR, and cross-sectional reconstruction images were used to observe and quantitatively measure the coronary artery stenosis caused by the calcified plaques. The lumen diameters at the most stenotic site and at both the proximal and distal ends of the stenosis were measured. Coronary artery stenosis >50% was considered to have obstructive coronary artery disease. The degree of coronary artery stenosis was calculated according to the following formula: [1–2 × the inner diameter of the narrowest lumen/(the normal lumen diameter proximal to the stenosis + the normal lumen diameter distal to the stenosis)] ×100%. According to the degree of coronary artery stenosis, coronary stenosis was divided into 5 grades: no stenosis; mild, 0%< coronary stenosis degree <50%; moderate, 50%< coronary stenosis degree <75%; severe, 75%< coronary stenosis degree <99%; and occlusion, 100%.

Histopathology

After CT enhancement scanning, coronary artery pathological section and staining were conducted within 24 hours. The coronary artery specimens were cut into 4-mm long segments and embedded in paraffin for pathological staining as the gold reference standard because pathological staining could directly detect the components of the specimen. In order to ensure that the patch of imaging scanning was the same patch for pathological section examination, the coronary tissue package was continuously sliced in 5–10 μm, and the distance between each slice and the coronary opening was recorded. Hematoxylin and eosin (HE) staining was performed. Two experimental workers who were blinded to the DSCT results observed the section with a fluorescence microscope (Olympus) under an ordinary light source, classified the pathological section, and took photos. When in disagreement, a third observer was consulted to reach a consensus. According to the criteria of the AHA (23), calcified plaques were defined as type Vb. Type V lesions are defined as lesions in which prominent new fibrous connective tissue has formed. A type V lesion in which the lipid core and other parts are calcified is referred to as a type Vb lesion. A lesion in which mineralization is the dominant feature is called type Vb or a calcified lesion. The degree of stenosis caused by each calcified plaque was measured, and the pathological classification and the measured degree of stenosis were used as the comparison criteria.

Statistical analysis

The statistical analysis was performed using the SPSS 17.0 software (IBM Corp., Armonk, NY, USA). To make the α error probability of 0.05 and a 95% statistical power, 34 arterial segments were needed. This study obtained 53 segments of the coronary artery and 69 plaques for analysis. All variables are expressed as ± standard deviation. The sensitivity was calculated to evaluate the detection ability of CT enhanced scans for calcified plaques. The CT value of calcified plaque was compared with that of the arterial lumen with the t-test. The Pearson test was used to evaluate the correlation between DSCT and the degree of coronary artery stenosis measured with pathology. The t-test was used to evaluate the difference between DSCT and the degree of coronary artery stenosis measured with pathology. Reliability was determined using intraclass correlation analyses. An intraclass correlation coefficient of >0.8 indicated excellent agreement. A P value <0.05 indicated statistical significance.

Results

Histopathology

Pathological staining detected 69 Vb plaques, including 43 plaques with mild calcification (calcification radian <90°; *Figure 2*, A1–B1), 12 with moderate calcification (90°< calcification arc <180°; *Figure 2*, A2–B2), and 14 with severe calcification (calcification arc >180°; *Figure 3*). The mean coronary artery stenosis caused by mild, moderate, and severe calcification was 22.1%±12.1%, 37.2%±16.8%, and 41.8%±15.9%, respectively (*Table 1*). The coronary artery stenosis was diagnosed as obstructive coronary artery disease on pathological staining in 35.7% (5/14) of severely calcified, 25% (3/12) of moderately calcified, and 4.6% (2/43) of mildly calcified plaques.

DSCT imaging

According to the 15 segment criteria of AHA, a computed tomography angiography (CTA) scan was completed in 84 segments, and 31 segments were excluded due to poor image quality or no pathological results for correlation analysis. Ultimately, 53 segments of coronary arteries were analyzed, including 22 segments of the right coronary artery, 23 segments of the left main coronary artery and anterior descending artery, and 8 segments of the left

Table 1 Coronary stenosis caused by plaques with different degrees of calcification

Calcification	Stenosis in CT	Stenosis in pathology	Differences between 2 measurements	P value
Mild	25.3%±11.8%	22.1%±12.1%	3.2%±2.0%	<0.001
Moderate	42.1%±16.0%	37.2%±16.8%	4.9%±4.7%	0.005
Severe	56.6%±17.9%	41.8%±15.9%	14.7%±8.2%	<0.001

CT, computed tomography.

Table 2 Detection of different calcified plaques with DSCT and pathology

DSCT	Pathology		
	Mild calcification	Moderate calcification	Severe calcification
Mild calcification	38	0	0
Moderate calcification	0	12	0
Severe calcification	0	0	14
Missed calcification	5	0	0
Sensitivity (95% CI)	88.3 (74.1–95.6%)	100% (69.8–100%)	100% (73.2–100%)

DSCT, dual-source computed tomography; 95% CI, 95% confidence interval.

Table 3 CT values of calcified plaques and contrast-enhanced arterial lumen

Variables	CT value	P value
Calcified plaques	253.3–577.7 (mean 393.2±104.1)	<0.001
Contrast-enhanced lumen	242.4–354.3 (mean 288.1±30.5)	

CT, computed tomography.

circumflex artery. DSCT detected 57 calcified lesions, including 31 mildly (*Figure 2*, A1), 12 moderately (*Figure 2*, A2), and 14 severely calcified lesions (*Figure 3*). Additionally, 7 Vb mildly calcified lesions were detected with DSCT but were not identified as calcified plaques with pathological staining, and 5 Vb mildly calcified plaques (*Figure 4*, A3–B3) were found with pathological staining but not detected with DSCT. The sensitivity of DSCT to detect mild, moderate, and severe Vb plaques was 88.3% [95% confidence interval (CI): 74.1–95.6%], 100% (95% CI: 69.8–100%), and 100% (95% CI: 73.2–100%), respectively (*Table 2*). A significant difference (P<0.001) was found in the mean CT value between the contrast-enhanced arterial lumen and calcified plaques (*Table 3*).

The mean value of coronary artery stenosis caused by mild, moderate, and severe calcified plaques measured on DSCT was 25.3%±11.8%, 42.1%±16.0%, and 56.6%±17.9%, respectively (*Table 1*). Excellent interobserver reproducibility of measurements of the coronary artery stenosis caused by the calcified plaques was obtained with the intraclass correlation coefficient of 0.992 (P<0.001). DSCT had a significant (P<0.001) correlation with pathological staining (R^2=0.9278, R^2=0.9158, R^2=0.7923, respectively) in quantifying coronary artery stenosis caused by mildly, moderately, and severely calcified plaques (*Figure 5*). Compared with pathological staining, DSCT overestimated coronary artery stenosis caused by plaques of mild (3.2%±2.0%; P<0.001), moderate (4.9%±4.7%; P=0.005), and severe calcification (14.7%±8.2%; P<0.001; *Table 1*). The accuracy of DSCT in quantifying coronary stenosis caused by mildly and moderately calcified plaques was higher than that caused by severely calcified plaques. DSCT could not qualitatively or quantitatively detect the fibrous cap of plaque or identify the location of calcified plaque in the wall (*Figures 3,4*).

Discussion

This study evaluated coronary arterial calcification in different forms on coronary CTA compared to histopathology. We
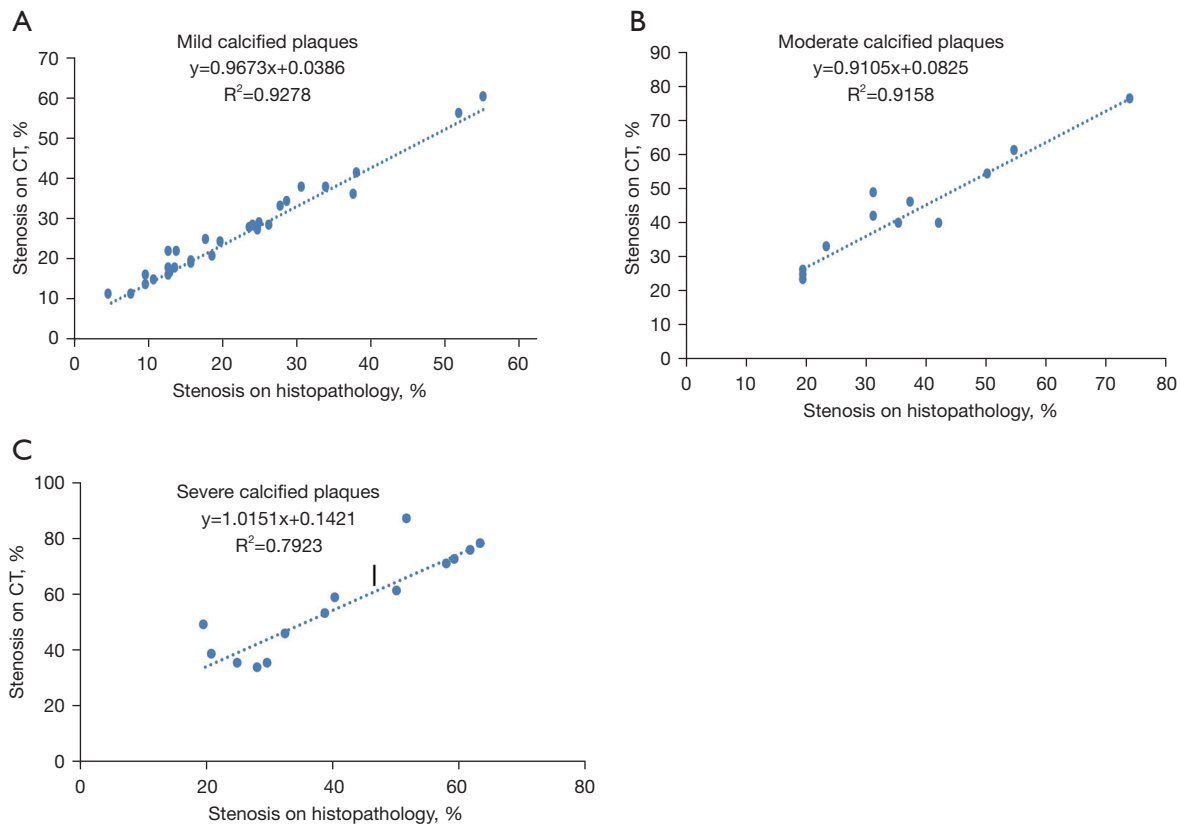
Figure 5 A good correlation was present between dual-source computed tomography (DSCT) and pathological staining in quantifying coronary stenosis. (A) A good correlation was present between DSCT imaging and pathological staining in mildly calcified plaques (R^2=0.9278; P<0.001). (B) A good correlation was present between DSCT imaging and pathological staining in moderately calcified plaques (R^2=0.9158; P<0.001). (C) A good correlation was present between DSCT imaging and pathological staining in severely calcified plaques (R^2=0.7923; P<0.001).

found that DSCT contrast enhancement scanning could detect and characterize coronary artery calcification, with a good correlation with histopathologic quantification of coronary artery stenosis caused by different types of calcified plaque, even though DSCT overestimated the stenosis. Coronary atherosclerotic plaques can be divided into calcified, noncalcified, and mixed on CT imaging according to the plaque composition. Early tiny calcifications are often accompanied by noncalcified plaques. However, due to the limited resolution of CT, these tiny calcifications are difficult to find. Most of the calcified plaques detected by CT are late atherosclerotic plaques with few or no noncalcified components. The main component of plaque is calcified, which causes arterial stenosis. In this study, only calcified plaques detected by CTA and pathology were analyzed, and noncalcified and mixed plaques were not

analyzed.

In our study, the sensitivity of DSCT in detecting mild, moderate, and severe Vb plaques was 88.3%, 100%, and 100%, respectively, indicating that DSCT has a high sensitivity for all types of calcified plaques. There was good consistency between CT value and pathological staining in identifying calcification, in line with the results of an *in vitro* study by Tanami *et al.* (19,24) and an *in vivo* study by Soeda *et al.* (25). Five Vb plaques of mild calcification were found with pathological staining but not with DSCT probably because these plaques were mainly microcalcifications at a deep location beyond the spatial resolution of DSCT. These plaques were not accompanied by atherosclerotic plaques and were relatively stable, with little impact on the patients. Some plaques of microcalcification which appear at the edge of advanced plaques or under the intima

with a thinned fibrous cap may increase the sheer force of the plaque, making the plaque unstable and prone to rupture, which may also be the reason why small plaques of microcalcification are closely related to acute coronary syndrome.

CT may have different accuracies in quantifying coronary stenosis caused by different types of calcified plaque (21,26). Our study demonstrated a good correlation between DSCT with pathology in quantifying coronary stenosis caused by mild, moderate, and severe calcification. Compared with pathology, DSCT overestimated coronary stenosis caused by mildly, moderately, and severely calcified plaques. The accuracy of DSCT in quantifying coronary stenosis caused by mildly and moderately calcified plaques is higher than that caused by severely calcified plaques. This may be because the partial volume effect caused by mildly and moderately calcified plaques is lighter than that caused by severely calcified plaques, which is similar to the finding of the *in vivo* study by Cerci *et al.* (26), who used 64-slice CT to investigate *in vivo* coronary stenosis. The *in vitro* study by Dettmer *et al.* (27), who used high-resolution CT in quantitative evaluation of percentage stenosis of coronary arteries, also reached a similar finding. Coronary artery calcification has typically been the main cause of quantitative coronary angiography misdiagnosing obstructive coronary artery disease.

Severe calcification often leads to poor image quality, making it impossible to evaluate arterial lumen stenosis. In order to avoid the missed diagnosis of patients, some clinicians consider coronary artery segments with severely calcified plaques that cannot be evaluated as having obstructive coronary arterial disease. However, our study revealed that although the degree of coronary stenosis caused by severely calcified plaques is higher than that caused by moderately or mildly calcified plaques, only 35.7% of coronary stenosis caused by severely calcified plaques is diagnosed as obstructive coronary artery stenosis on pathological staining, which suggests that severely calcified plaques do not necessarily lead to severe coronary artery stenosis. Sangiorgi *et al.* (10) also believed that the quantification of mural calcification could not be used to predict lumen narrowing, even though the amount of calcification correlates well with the overall magnitude of atherosclerotic plaque burden. This finding is also why some believe extensive calcification may be a protective mechanism for patients with coronary heart disease, as extensive calcification may make the plaques stable and not prone to atherosclerotic coronary syndrome.

Nonetheless, severe calcification often indicates that patients have a serious load of atherosclerotic plaque, and the stenosis caused by severe calcification often makes the coronary artery lumen stiff, leading to poor distal coronary perfusion and even symptoms of heart failure. Therefore, the segments with poor image quality caused by severe calcification should not be considered as having obstructive coronary artery disease. Nevertheless, the severe and diffuse calcified coronary artery is the primary reason for difficult coronary bypass surgery and poor prognosis of percutaneous coronary intervention (12,14,28). Coronary endarterectomy is usually necessary for extensive diffuse calcified coronary arteries and may result in an increased risk of acute thrombosis and coronary artery rupture following coronary bypass surgery. Extensive and severe calcification of the coronary artery may lead to poor stent expansion after percutaneous coronary intervention and increase the risk of restenosis. Accurate quantification of severe coronary artery calcification will be of great significance in guiding the classification of patients with coronary heart disease and devising strategies for percutaneous coronary intervention or bypass surgery (15,29-31).

In our study, only 4.6% of mildly and 25% of moderately calcified plaques were diagnosed as obstructive coronary artery disease. Mildly and moderately calcified plaques may not be able to cause severe coronary artery stenosis. In our study, DSCT detected two calcified plaques in the same cross section. These two calcified plaques led to severe arterial stenosis. Pathological staining suggested that the larger calcified plaque might be the main cause of arterial lumen stenosis. Although a smaller calcified plaque has less effect on the stenosis, it has a thinner fibrous cap and uneven calcified density, which may break and cause plaque rupture and acute coronary artery syndrome. This may be why mildly and moderately calcified plaques are more dangerous. Furthermore, calcified plaques are usually accompanied by atherosclerotic plaques at different stages of coronary atherosclerosis, and mildly and moderately calcified plaques may be accompanied by early fibroatherosclerotic plaques with a core rich in lipids, which is why these calcified plaques pose a greater threat (32,33).

Coronary calcification can occur at different locations in the coronary artery wall (34,35) and may have different influences on the patient in regard to the progression of coronary atherosclerosis. The relationship between the location of calcified plaques and cardiac events has been less studied in the clinic and is not clear. Intimal calcification of the coronary artery may cause a higher possibility of arterial

stenosis and plaque rupture. In contrast, calcification at the junction of the adventitia and media is more likely to results in positive vascular remodeling. In our study, DSCT detected multiple calcified plaques at the same level, whose locations in the arterial wall were revealed with pathological staining rather than with DSCT which has limited spatial resolution.

In our study, 10% formalin-soaked coronary arteries were used as the experimental object, which could prevent the influence of formalin on arterial lumen stenosis in pathological sections and ensure the consistency of coronary artery stenosis measured with coronary CTA and pathological staining. This approach was different from that in the study by Dettmer *et al.* (27), who injected iodinated contrast media into the coronary artery (not fixed with formalin) for investigation. In addition, in our study, serial pathological sections were collected from the coronary arteries, and the number of plaques found in these serial sections was compared to that detected with DSCT. The study by Henzler *et al.* (24) used the number of plaques observed by coronary artery dissection as the comparison standard. The approach in our study is more accurate and reliable than using the number of plaques observed with coronary artery dissection as the comparison standard.

Our study used isolated coronary arteries and DSCT to retrospectively compare, qualitatively and quantitatively, the sensitivity and correlation of coronary CTA with those of histopathology in assessing coronary arterial calcification in comparison with histopathology. The advantage of using the isolated coronary arteries and DSCT, as compared to CT, lies in the accurate detection and analysis of the histopathological changes. DSCT has a high temporal and spatial resolution and has been widely used as a noninvasive means to evaluate coronary heart disease. However, coronary atherosclerosis caused by calcified plaque (especially microcalcification, calcification mass, severe diffuse calcification, or chronic calcification plaque occlusion) is still the main criterion for coronary heart disease classification and determining bypass surgery, interventional surgery, and patient prognosis.

This study evaluated the accuracy of qualitative and quantitative coronary atherosclerotic plaque with pathology as the standard, providing a theoretical basis for the clinical application of DSCT to evaluate calcified coronary plaque and guide patient treatment. Invasive angiography as an invasive examination method is considered the gold standard for diagnosing coronary heart disease, but it can only display the stenosis caused by calcified plaque in 2-dimensional images and cannot quantitatively evaluate calcified plaque in 3-dimensional images. Due to the influence of calcification artifacts, invasive angiography has certain limitations in evaluating calcified plaque. Intravascular ultrasound (IVUS), as an invasive test, can evaluate calcified plaque. However, due to the influence of calcified plaque on IVUS penetration and the influence of calcified sound and shadow, IVUS cannot accurately and quantitatively evaluate the thickness and volume of coronary artery calcified plaque. As an invasive examination, optical coherence tomography (OCT) can evaluate calcified plaque with a resolution of 10–20 μm, so it can accurately identify and quantify coronary artery calcified plaque. However, due to its limited horizontal resolution, it cannot evaluate the volume and thickness of larger calcified plaque.

Moreover, IVUS and OCT are expensive and cannot be widely applied for clinical screening. As a noninvasive examination, DSCT can both identify and quantify coronary artery calcified plaque, and coronary CTA has been recognized as a first-line approach for assessing coronary artery disease in professional societal guidelines and proper use criteria (36). Our study provides a theoretical basis for the clinical diagnosis and evaluation of coronary artery calcified plaque with CTA to reduce misdiagnosis and missed diagnoses in clinical practice. Although coronary CTA may result in the overestimation of coronary diseases by clinical readers, the quantitative coronary CTA data can be used in machine learning as a useful tool to improving the accuracy of CTA evaluation of coronary disease. Machine learning has shown promising outcomes in automated identification and the exclusion of atherosclerotic coronary artery stenoses on coronary CTA in combination with specialized software (37-39). A novel artificial intelligence–based evaluation of coronary CTA has been demonstrated to enable rapid and accurate identification and exclusion of high-grade stenosis of a coronary artery caused by atherosclerotic plaques with less reader variability (36). Moreover, specialized software algorithms such as that developed by the Elucid Bioimaging company can be used to quantitatively process and determine the characteristics of coronary plaque tissues using conventional CTA data sets, with a lower reader variability (39). In the future, the combination of artificial intelligence, software algorithms, big data, and CTA data is expected to be widely applied in clinical practice to accurately evaluate coronary disease.

Some limitations may exist in our study. First, the experiment was carried out in the static condition *in vitro*, with no effect of cardiac motion artifact or the influence

of surrounding tissue of the thoracic cavity and coronary artery being considered. Second, the specimens were taken from corpses and soaked in formalin before DSCT enhanced scanning, which might have altered the plaque density. Third, in scanning the arteries in vitro, the imaging obtained differed from that obtained *in vivo* in terms of image quality and scattered radiation. In addition, only coarse contrast-enhanced coronary angiography and segments with good imaging were selected for analysis. The scanning parameters of coronary CTA in this experiment were relatively high, which might have affected the outcome of this experiment. Finally, this was merely an *in vitro* study which included a small sample size. These limitations mean that the direct clinical application of the study outcomes cannot be guaranteed and that interpretation of these outcomes should be restrained.

In conclusion, DSCT contrast enhancement scanning may be used to detect and characterize coronary artery calcification and shows good correlation with histopathologic quantification of coronary artery stenosis caused by different types of calcified plaques, even though coronary CTA may overestimate the stenosis.

Acknowledgments

Footnote

Reporting Checklist: The authors have completed the STARD (Standards for the Reporting of Diagnostic accuracy studies) reporting checklist. Available at https://qims.amegroups. com/article/view/10.21037/qims-22-603/rc

Conflicts of Interest: All authors have completed the ICMJE uniform disclosure form (available at https://qims. amegroups.com/article/view/10.21037/qims-22-603/coif). The authors have no conflicts of interest to declare.

Ethical Statement: The authors are accountable for all aspects of the work in ensuring that questions related to the accuracy or integrity of any part of the work are appropriately investigated and resolved. The study was conducted in accordance with the Declaration of Helsinki (as revised in 2013). This retrospective study was approved by the ethics committee of The First Affiliated Hospital of Zhengzhou University (No. 20201252), and individual consent for this retrospective analysis was waived.

References

1. Budoff MJ, Young R, Burke G, Jeffrey Carr J, Detrano RC, Folsom AR, Kronmal R, Lima JAC, Liu KJ, McClelland RL, Michos E, Post WS, Shea S, Watson KE, Wong ND. Ten-year association of coronary artery calcium with atherosclerotic cardiovascular disease (ASCVD) events: the multi-ethnic study of atherosclerosis (MESA). Eur Heart J 2018;39:2401-8.

2. Peng AW, Dardari ZA, Blumenthal RS, Dzaye O, Obisesan OH, Iftekhar Uddin SM, Nasir K, Blankstein R, Budoff MJ, Bødtker Mortensen M, Joshi PH, Page J, Blaha MJ. Very High Coronary Artery Calcium (≥1000) and Association With Cardiovascular Disease Events, Non-Cardiovascular Disease Outcomes, and Mortality: Results From MESA. Circulation 2021;143:1571-83.

3. Budoff MJ, Young R, Lopez VA, Kronmal RA, Nasir K, Blumenthal RS, Detrano RC, Bild DE, Guerci AD, Liu K, Shea S, Szklo M, Post W, Lima J, Bertoni A, Wong ND. Progression of coronary calcium and incident coronary heart disease events: MESA (Multi-Ethnic Study of Atherosclerosis). J Am Coll Cardiol 2013;61:1231-9.

4. Wang W, Yang L, Wang S, Wang Q, Xu L. An automated quantification method for the Agatston coronary artery calcium score on coronary computed tomography angiography. Quant Imaging Med Surg 2022;12:1787-99.

5. Dai X, Lu Z, Yu Y, Yu L, Xu H, Zhang J. The use of lesion-specific calcium morphology to guide the appropriate use of dynamic CT myocardial perfusion imaging and CT fractional flow reserve. Quant Imaging Med Surg 2022;12:1257-69.

6. Saita T, Fujii K, Hao H, Imanaka T, Shibuya M, Fukunaga M, Miki K, Tamaru H, Horimatsu T, Nishimura M, Sumiyoshi A, Kawakami R, Naito Y, Kajimoto N, Hirota S, Masuyama T. Histopathological validation of optical frequency domain imaging to quantify various types of coronary calcifications. Eur Heart J Cardiovasc Imaging 2017;18:342-9.

7. Burke AP, Weber DK, Kolodgie FD, Farb A, Taylor AJ, Virmani R. Pathophysiology of calcium deposition in coronary arteries. Herz 2001;26:239-44.

8. Pu J, Mintz GS, Biro S, Lee JB, Sum ST, Madden SP, Burke AP, Zhang P, He B, Goldstein JA, Stone GW, Muller JE, Virmani R, Maehara A. Insights into echo-attenuated plaques, echolucent plaques, and plaques with spotty calcification: novel findings from comparisons among intravascular ultrasound, near-infrared spectroscopy, and pathological histology in 2,294 human coronary artery segments. J Am Coll Cardiol 2014;63:2220-33.

9. Torii S, Sato Y, Otsuka F, Kolodgie FD, Jinnouchi H, Sakamoto A, et al. Eruptive Calcified Nodules as a Potential Mechanism of Acute Coronary Thrombosis and Sudden Death. J Am Coll Cardiol 2021;77:1599-611.

10. Sangiorgi G, Rumberger JA, Severson A, Edwards WD, Gregoire J, Fitzpatrick LA, Schwartz RS. Arterial calcification and not lumen stenosis is highly correlated with atherosclerotic plaque burden in humans: a histologic study of 723 coronary artery segments using nondecalcifying methodology. J Am Coll Cardiol 1998;31:126-33.

11. Mori H, Torii S, Kutyna M, Sakamoto A, Finn AV, Virmani R. Coronary Artery Calcification and its Progression: What Does it Really Mean? JACC Cardiovasc Imaging 2018;11:127-42.

12. Ertelt K, Généreux P, Mintz GS, Reiss GR, Kirtane AJ, Madhavan MV, Fahy M, Williams MR, Brener SJ, Mehran R, Stone GW. Impact of the severity of coronary artery calcification on clinical events in patients undergoing coronary artery bypass grafting (from the Acute Catheterization and Urgent Intervention Triage Strategy Trial). Am J Cardiol 2013;112:1730-7.

13. Copeland-Halperin RS, Baber U, Aquino M, Rajamanickam A, Roy S, Hasan C, Barman N, Kovacic JC, Moreno P, Krishnan P, Sweeny JM, Mehran R, Dangas G, Kini AS, Sharma SK. Prevalence, correlates, and impact of coronary calcification on adverse events following PCI with newer-generation DES: Findings from a large multiethnic registry. Catheter Cardiovasc Interv

2018;91:859-66.

14. Kawashima H, Serruys PW, Hara H, Ono M, Gao C, Wang R, Garg S, Sharif F, de Winter RJ, Mack MJ, Holmes DR, Morice MC, Kappetein AP, Thuijs DJFM, Milojevic M, Noack T, Mohr FW, Davierwala PM, Onuma Y; . 10-Year All-Cause Mortality Following Percutaneous or Surgical Revascularization in Patients With Heavy Calcification. JACC Cardiovasc Interv 2022;15:193-204.

15. Bourantas CV, Zhang YJ, Garg S, Mack M, Dawkins KD, Kappetein AP, Mohr FW, Colombo A, Holmes DR, Ståhle E, Feldman T, Morice MC, de Vries T, Morel MA, Serruys PW. Prognostic implications of severe coronary calcification in patients undergoing coronary artery bypass surgery: an analysis of the SYNTAX study. Catheter Cardiovasc Interv 2015;85:199-206.

16. Vonder M, Pelgrim GJ, Huijsse SEM, Haubenreisser H, Meyer M, van Ooijen PMA, Oudkerk M, Henzler T, Vliegenthart R. Coronary artery calcium quantification on first, second and third generation dual source CT: A comparison study. J Cardiovasc Comput Tomogr 2017;11:444-8.

17. Schicchi N, Fogante M, Pirani PE, Agliata G, Piva T, Tagliati C, Marcucci M, Francioso A, Giovagnoni A. Third generation dual source CT with ultra-high pitch protocol for TAVI planning and coronary tree assessment: feasibility, image quality and diagnostic performance. Eur J Radiol 2020;122:108749.

18. Austen WG, Edwards JE, Frye RL, Gensini GG, Gott VL, Griffith LS, McGoon DC, Murphy ML, Roe BB. A reporting system on patients evaluated for coronary artery disease. Report of the Ad Hoc Committee for Grading of Coronary Artery Disease, Council on Cardiovascular Surgery, American Heart Association. Circulation 1975;51:5-40.

19. Tanami Y, Ikeda E, Jinzaki M, Satoh K, Nishiwaki Y, Yamada M, Okada Y, Kuribayashi S. Computed tomographic attenuation value of coronary atherosclerotic plaques with different tube voltage: an ex vivo study. J Comput Assist Tomogr 2010;34:58-63.

20. Achenbach S, Moselewski F, Ropers D, Ferencik M, Hoffmann U, MacNeill B, Pohle K, Baum U, Anders K, Jang IK, Daniel WG, Brady TJ. Detection of calcified and noncalcified coronary atherosclerotic plaque by contrast-enhanced, submillimeter multidetector spiral computed tomography: a segment-based comparison with intravascular ultrasound. Circulation 2004;109:14-7.

21. Vavere AL, Arbab-Zadeh A, Rochitte CE, Dewey M,

Niinuma H, Gottlieb I, Clouse ME, Bush DE, Hoe JW, de Roos A, Cox C, Lima JA, Miller JM. Coronary artery stenoses: accuracy of 64-detector row CT angiography in segments with mild, moderate, or severe calcification--a subanalysis of the CORE-64 trial. Radiology 2011;261:100-8.

22. Ehara S, Kobayashi Y, Yoshiyama M, Shimada K, Shimada Y, Fukuda D, Nakamura Y, Yamashita H, Yamagishi H, Takeuchi K, Naruko T, Haze K, Becker AE, Yoshikawa J, Ueda M. Spotty calcification typifies the culprit plaque in patients with acute myocardial infarction: an intravascular ultrasound study. Circulation 2004;110:3424-9.

23. Stary HC, Chandler AB, Dinsmore RE, Fuster V, Glagov S, Insull W Jr, Rosenfeld ME, Schwartz CJ, Wagner WD, Wissler RW. A definition of advanced types of atherosclerotic lesions and a histological classification of atherosclerosis. A report from the Committee on Vascular Lesions of the Council on Arteriosclerosis, American Heart Association. Circulation 1995;92:1355-74.

24. Henzler T, Porubsky S, Kayed H, Harder N, Krissak UR, Meyer M, Sueselbeck T, Marx A, Michaely H, Schoepf UJ, Schoenberg SO, Fink C. Attenuation-based characterization of coronary atherosclerotic plaque: comparison of dual source and dual energy CT with single-source CT and histopathology. Eur J Radiol 2011;80:54-9.

25. Soeda T, Uemura S, Morikawa Y, Ishigami K, Okayama S, Hee SJ, Nishida T, Onoue K, Somekawa S, Takeda Y, Kawata H, Horii M, Saito Y. Diagnostic accuracy of dual-source computed tomography in the characterization of coronary atherosclerotic plaques: comparison with intravascular optical coherence tomography. Int J Cardiol 2011;148:313-8.

26. Cerci R, Vavere AL, Miller JM, Yoneyama K, Rochitte CE, Dewey M, Niinuma H, Clouse ME, Laham R, Bush DE, Shapiro EP, Lardo AC, Cox C, Brinker J, Lima JA, Arbab-Zadeh A. Patterns of coronary arterial lesion calcification by a novel, cross-sectional CT angiographic assessment. Int J Cardiovasc Imaging 2013;29:1619-27.

27. Dettmer M, Glaser-Gallion N, Stolzmann P, Glaser-Gallion F, Fornaro J, Feuchtner G, Jochum W, Alkadhi H, Wildermuth S, Leschka S. Quantification of coronary artery stenosis with high-resolution CT in comparison with histopathology in an ex vivo study. Eur J Radiol 2013;82:264-9.

28. Hoffmann R, Mintz GS, Popma JJ, Satler LF, Kent KM, Pichard AD, Leon MB. Treatment of calcified coronary lesions with Palmaz-Schatz stents. An intravascular ultrasound study. Eur Heart J 1998;19:1224-31.

29. Kobayashi Y, Okura H, Kume T, Yamada R, Kobayashi Y, Fukuhara K, Koyama T, Nezuo S, Neishi Y, Hayashida A, Kawamoto T, Yoshida K. Impact of target lesion coronary calcification on stent expansion. Circ J 2014;78:2209-14.

30. Madhavan MV, Tarigopula M, Mintz GS, Maehara A, Stone GW, Généreux P. Coronary artery calcification: pathogenesis and prognostic implications. J Am Coll Cardiol 2014;63:1703-14.

31. Zhang M, Matsumura M, Usui E, Noguchi M, Fujimura T, Fall KN, Zhang Z, Nazif TM, Parikh SA, Rabbani LE, Kirtane AJ, Collins MB, Leon MB, Moses JW, Karmpaliotis D, Ali ZA, Mintz GS, Maehara A. Intravascular Ultrasound-Derived Calcium Score to Predict Stent Expansion in Severely Calcified Lesions. Circ Cardiovasc Interv 2021;14:e010296.

32. Kataoka Y, Wolski K, Uno K, Puri R, Tuzcu EM, Nissen SE, Nicholls SJ. Spotty calcification as a marker of accelerated progression of coronary atherosclerosis: insights from serial intravascular ultrasound. J Am Coll Cardiol 2012;59:1592-7.

33. Nakahara T, Dweck MR, Narula N, Pisapia D, Narula J, Strauss HW. Coronary Artery Calcification: From Mechanism to Molecular Imaging. JACC Cardiovasc Imaging 2017;10:582-93.

34. Demer LL, Tintut Y. Vascular calcification: pathobiology of a multifaceted disease. Circulation 2008;117:2938-48.

35. Otsuka F, Sakakura K, Yahagi K, Joner M, Virmani R. Has our understanding of calcification in human coronary atherosclerosis progressed? Arterioscler Thromb Vasc Biol 2014;34:724-36.

36. Griffin WF, Choi AD, Riess JS, Marques H, Chang HJ, Choi JH, et al. AI Evaluation of Stenosis on Coronary CT Angiography, Comparison With Quantitative Coronary Angiography and Fractional Flow Reserve: A CREDENCE Trial Substudy. JACC Cardiovasc Imaging 2022. [Epub ahead of print]. pii: S1936-878X(22)00001-8. doi: 10.1016/j.jcmg.2021.10.020.

37. Choi AD, Marques H, Kumar V, Griffin WF, Rahban H, Karlsberg RP, Zeman RK, Katz RJ, Earls JP. CT Evaluation by Artificial Intelligence for Atherosclerosis, Stenosis and Vascular Morphology (CLARIFY): A Multi-center, international study. J Cardiovasc Comput Tomogr 2021;15:470-6.

38. Stuijfzand WJ, van Rosendael AR, Lin FY, Chang HJ, van den Hoogen IJ, Gianni U, et al. Stress Myocardial

Perfusion Imaging vs Coronary Computed Tomographic Angiography for Diagnosis of Invasive Vessel-Specific Coronary Physiology: Predictive Modeling Results From the Computed Tomographic Evaluation of Atherosclerotic Determinants of Myocardial Ischemia (CREDENCE) Trial. JAMA Cardiol 2020;5:1338-48.

39. Sheahan M, Ma X, Paik D, Obuchowski NA, St Pierre S, Newman WP 3rd, Rae G, Perlman ES, Rosol M, Keith JC Jr, Buckler AJ. Atherosclerotic Plaque Tissue: Noninvasive Quantitative Assessment of Characteristics with Software-aided Measurements from Conventional CT Angiography. Radiology 2018;286:622-31.